Chapter 7
Green 5G Femtocells for Supporting Indoor Generated IoT Traffic

Elias Yaacoub

Abstract Supporting the traffic emanating from the internet of things (IoT) is a major challenge for 5G systems. A significant portion of this traffic will be generated indoors. Therefore, in this chapter, femtocell networks designed for supporting IoT traffic are studied. A deployment scenario of femtocell networks with centralized control is investigated. It consists of an integrated wired/wireless system, where the femtocell access points (FAPs) are controlled by a single entity. This permits performing joint radio resource management in a centralized and controlled way in order to enhance the quality of service performance for all users in the network. It also allows an energy efficient operation of the network by switching off redundant femtocells whenever possible. Two algorithms are proposed and analyzed. The first one is a utility maximizing radio resource management algorithm, whereas the second one is a FAP switch off algorithm, implemented at the central controller. The joint wired/wireless resource management approach is compared to the distributed resource management case, where each femtocell acts as an independent wireless network unaware of the channel and interference conditions with the other cells. The proposed algorithm was shown to lead to significant gains. Furthermore, considerable energy savings were obtained with the green algorithm.

7.1 Introduction

One of the major challenges for 5G cellular systems is the capability to support the machine-to-machine (M2M) traffic with the Internet of Things (IoT) becoming a reality. In fact, IoT is expected to include billions of connected devices using M2M communications [1]. These devices will have a variety of requirements and different types of behavior in the network. For example, certain devices will access

Elias Yaacoub
Strategic Decisions Group (SDG) and Arab Open University (AOU), Beirut, Lebanon, e-mail: eliasy@ieee.org

the network frequently and periodically to transmit short amounts of data, such as smart meters used for advanced metering infrastructure (AMI) in the smart grid [2, 3]. Other devices can store data measurements and transmit in bulk, unless there is an alerting situation, such as sensor networks for environment monitoring [4]. In fact, wireless sensor networks (WSNs) will constitute an integral part of the IoT paradigm, spanning different application areas including environment, smart grid, vehicular communication, and agriculture, among others [5]. Solutions to meet the increasing demand include the deployment of heterogeneous networks involving macrocells and small cells (picocells, femtocells, etc.), distributed antenna systems (DAS), or relay stations (RSs).

A significant portion of IoT traffic will be generated indoors. This includes data from smart meters (for electricity, water, etc.), from monitoring sensors (e.g., for temperature, pollution levels inside an apartment or building, among other measurements), and for home automation systems. IoT traffic can also emanate from m-Health applications, with sensors relaying their monitoring data of elderly people or indoor patients to the appropriate medical personnel and health centers [6]. Femtocell Access Points (FAPs) can be used to handle this indoor traffic and reduce the load on macrocell base stations (BSs). They generally consist of small, low power, plug and play devices providing indoor wireless coverage to meet the quality of service (QoS) requirements for indoor data users [7]. FAPs are installed inside the home or office of a given subscriber. They are connected to the mobile operator's core network via wired links, e.g. digital subscriber line (DSL) [8]. However, they are not under the direct control of the mobile operator since they are not connected to neighboring macrocell BSs (MBSs) through the standardized interfaces, e.g., the X2 interface for the long term evolution (LTE) cellular system.

This chapter investigates the case of 5G IoT in indoor scenarios, where the deployment of FAPs is used to transmit the IoT traffic. Radio resource management (RRM) algorithms are proposed for optimizing the resource allocation process and meeting the quality of service (QoS) requirements of the IoT applications. Furthermore, techniques for the green operation of femtocell networks are proposed, with the objective of maintaining QoS while ensuring an energy efficient operation of the network.

The chapter is organized as follows. Femtocell networks are overviewed in Section 7.2. The system model is presented in Section 7.3. The utility metrics leading to different QoS and performance targets are described in Section 7.4. The joint RRM algorithm implemented at the central controller is presented in Section 7.5, and the FAP on/off switching algorithm is presented in Section 7.6. Simulation results are presented and analyzed in Section 7.7. Finally, conclusions are drawn in Section 7.8.

7.2 Overview of Femtocell Networks

The proliferation of small cells, notably femtocells, is expected to increase in the coming years [9]. Since most of the wireless traffic is initiated indoors, FAPs are

designed to handle this traffic and reduce the load on MBSs by providing indoor wireless coverage to meet QoS requirements for indoor data users [7]. Since FAPs are not under the direct control of the mobile operator and do not use the LTE X2 interface to connect to other BSs, they pose several challenges to network operation and management.

A major challenge is that the overall interference levels in the network depend on the density of small cells and their operation, which affects the configuration of macrocell sites [10]. In [11], this problem was addressed by proposing macrocell-femtocell cooperation, where a femtocell user may act as a relay for macrocell users, and in return each cooperative macrocell user grants the femtocell user a fraction of its superframe. In [12], it was assumed that both macrocells and small cells are controlled by the same operator, and it was shown that in this case the operator can control the system loads by tuning the pricing and the bandwidth allocation policy between macrocells and small cells.

On the other hand, other works investigated radio resource management (RRM) in femtocell networks by avoiding interference to/from macrocells. Most of these works focused on using cognitive radio (CR) channel sensing techniques to determine channel availability. In [13], the femtocell uses cognitive radio to sense the spectrum and detect macrocell transmissions to avoid interference. It then performs radio resource management on the free channels. However, there is a time dedicated for sensing the channel that cannot overlap with transmission/RRM time. A channel sensing approach for improving the capacity of femtocell users in macro-femto overlay networks is proposed in [14]. It is based on spatial radio resource reuse based on the channel sensing outcomes. In [15], enhanced spectrum sensing algorithms are proposed for femtocell networks in order to ensure better detection accuracy of channels occupied by macrocell traffic.

In this chapter, LTE femtocell networks are investigated. FAPs are not assumed to be controlled by the mobile operator. However, in certain scenarios, FAPs at a given location can be controlled by a single entity. This can happen, for example, in a university campus, hotel, housing complex, or office building. In such scenarios, in addition to the wireless connection between FAPs and mobile terminals, FAPs can be connected via a wired high-speed network to a central controller within the building or campus. This can allow more efficient RRM decisions leading to significant QoS enhancements for mobile users. Furthermore, it can allow energy efficient operation of the network, by switching off unnecessary FAPs whenever possible, and serving their active femto user equipment (FUEs) from other neighboring FAPs that still can satisfy their QoS requirements. Due to centralized control, users do not have to worry about opening the access to their FAPs for FUEs within the premises, since the controller will guarantee the QoS. This scenario is studied in this chapter, where two algorithms are presented: A utility maximizing RRM algorithm to perform resource allocation over the FAPs controlled by the same entity, and an algorithm for the green operation of LTE femtocell networks via on/off switching. Significant gains are shown to be achieved under this integrated wired/wireless scenario compared to the case where each FAP acts independently.

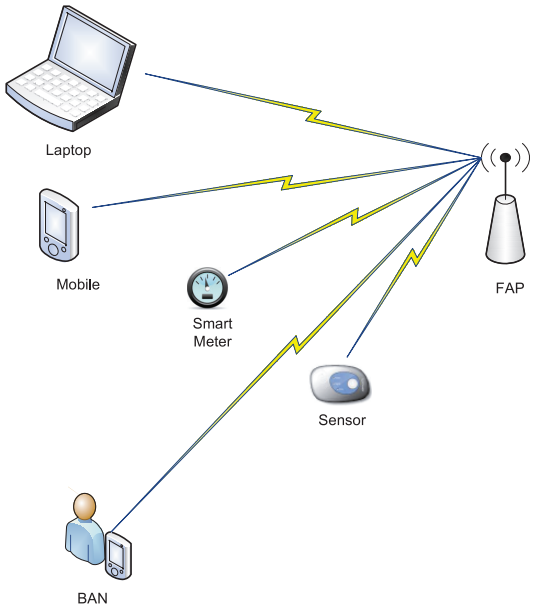

Fig. 7.1 Connections between a FAP and different IoT devices.

7.3 System Model

Fig. 7.1 shows multiple IoT devices that can be found indoors. They include smart meters (for utilities: electricity, water, gas), sensors (for monitoring temperature, humidity, environment parameters, or the performance of electrical appliances for example), and body area networks (BANs) formed by sensors used to monitor a human being's vital parameters for m-Health applications. The sensors of a BAN can send this information via short range communications to the person's mobile phone. These IoT devices can communicate with the network through various technologies such as Bluetooth, Zigbee, or WiFi. In the case of BAN, the sensors actually use these technologies to communicate with the patient's smart phone, which in turn communicates with the access point. With the deployment of 5G and the expected proliferation of IoT devices, these indoor devices can communicate with an

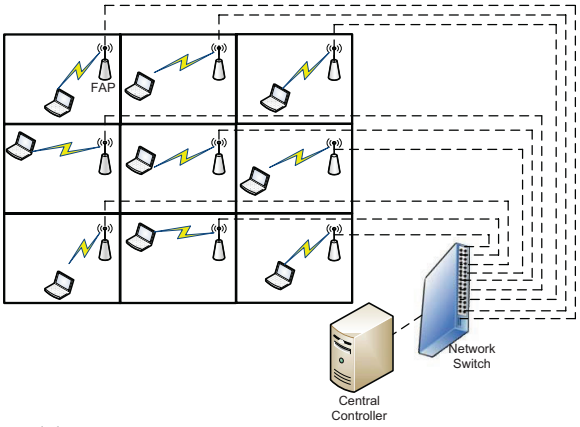

Fig. 7.2 System model.

indoor FAP using the cellular technology. With LTE-Advanced (LTE-A), this can take place using device-to-device (D2D) communications for example. Similarly, other devices such as laptops and mobile phones can still use the FAP normally, as shown in Fig. 7.1. This allows these devices to benefit from advanced 5G features guaranteeing QoS levels, and provides an integrated wireless network indoors without incurring any additional costs, since the indoor communications between IoT devices and the 5G FAP can be free of charge, similarly to Bluetooth or WiFi communications. This comes at no loss for cellular operators too, since FAPs are user installed devices and they relief the MBSs from this indoor generated traffic.

In this chapter, we consider a worst case scenario of a single device connected to a FAP, and located at the opposite extremity from that FAP inside the house or apartment. We also assume that the data rate requested by this device is equal to or larger than the aggregate data rates of several IoT devices and other devices. For example, real-time smart meter readings require a data rate of around 64 kbps [3], whereas the data rates considered in the simulations of this chapter are orders of magnitude larger (on the order of several Mbps). This allows simplifying the simulations without losing the insights from the approach, since a worst case scenario is adopted.

The system model of the worst case scenario with a single device per apartment, denoted as the femto user equipment (FUE) is shown in Fig. 7.2. As an example, a building having three apartments per floor is considered. One FAP is available in each apartment, primarily to serve the FUEs available in that apartment. The FAPs are connected to FUEs over the air interface, but they are connected via a wired network (dashed lines in Fig. 7.2) to a central controller located within the building (for example, in a room hosting telecom/networking equipment in the basement).

Interference is caused by the transmissions of a FAP to the FUEs served by the other FAPs in other apartments. In the downlink (DL) direction from the FAPs to the

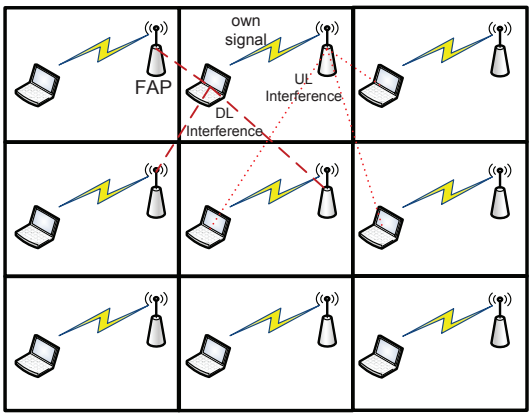

Fig. 7.3 Intercell interference in the uplink and downlink.

FUEs, interference is caused by the transmissions of a FAP to the FUEs served by the other FAPs in other apartments, as shown by the dashed lines in Fig. 7.3, representing the interference on the FUE in the second apartment in the third floor from the FAPs in neighboring apartments. In the uplink (UL) direction from the FUEs to the FAPs, interference is caused by the transmissions of an FUE to the FAPs in other apartments, as shown by the dotted lines in Fig. 7.3, representing the interference on the second FAP in the third floor from the FUEs in neighboring apartments. Centralized RRM in an integrated wired/wireless scenario, as shown in Fig. 7.2, can be used to mitigate the impact of interference and enhance QoS performance. In addition, centralized control allows to switch certain FAPs off, or put them in sleep mode, when they are not serving any FUEs, or when the FUEs they serve can be handed over to other neighboring FAPs within the same building, without affecting their QoS. An algorithm to implement this green switching approach is one of the main contributions of this chapter, and is presented in Section 7.6.

In the absence of the central controller and wired connections between FAPs, each FAP would act independently, without being aware of the network conditions within the coverage areas of other FAPs. Thus, each FAP would selfishly serve its own FUEs, regardless of the interference caused to other FUEs, or the redundant energy consumption.

The building of Fig. 7.2 is assumed to be within the coverage area of an MBS, positioned at a distance d_{BS} from the building. The interference from the MBS to the FAPs is taken into account in the analysis: it is assumed in this chapter that the MBS is fully loaded, i.e. all its resource blocks (RBs) are occupied, which causes macro interference to all the FAPs in the building. No coordination is assumed between the mobile operator of the MBS and the central controller of the building FAPs.

Energy efficient FAP switching in conjunction with intelligent RRM is considered in this chapter within the framework of LTE. The downlink direction (DL) from the FAPs to the FUEs is studied, although the presented approach can be easily adapted to the uplink (UL) direction from the FUEs to the FAPs. In LTE, orthogonal frequency division multiple access (OFDMA) is the access scheme used for DL communications. The spectrum is divided into RBs, with each RB consisting of 12 adjacent subcarriers. The assignment of an RB takes place every 1 ms, which is the duration of one transmission time interval (TTI), or, equivalently, the duration of two 0.5 ms slots [16, 17]. LTE allows bandwidth scalability, where a bandwidth of 1.4, 3, 5, 10, 15, and 20 MHz corresponds to 6, 15, 25, 50, 75, and 100 RBs, respectively [17]. In this chapter, scenarios where the MBS and the FAPs are using the same bandwidth are assumed (i.e. a frequency reuse of one where bandwidth chunks in different cells are not orthogonal).

7.3.1 Channel Model

The pathloss between FUE k_l (connected to FAP l) and FAP j is given by [18]:

$$\begin{aligned} PL_{k_l,j,\mathrm{dB}} =& 38.46 + 20\log_{10} d_{k_l,j} + 0.3 d_{k_l,j} \\ &+ 18.3 n^{((n+2)/(n+1)-0.46)} + qL_{\mathrm{iw}} \end{aligned} \tag{7.1}$$

where $d_{k_l,j}$ is the indoor distance between FUE k_l and FAP j, n is the number of floors separating FUE k_l and FAP j, q is the number of walls between apartments, and L_{iw} is a per wall penetration loss. In (7.1), the first term $38.46 + 20\log_{10} d_{k_l,j}$ is the distance dependent free space path loss, the term $0.3 d_{k_l,j}$ models indoor distance dependent attenuation, the term $18.3 n^{((n+2)/(n+1)-0.46)}$ indicates losses due to propagation across floors, and qL_{iw} corresponds to losses across apartment walls in the same floor. In this chapter, $L_{\mathrm{iw}} = 5$ dB is used as recommended in [18]. The pathloss between FUE k_l and its serving FAP l is a special case of (7.1), with $j = l$, $n = 0$, and $q = 0$.

The FAPs in this chapter are assumed to be numbered from $j = 1$ to $j = L$, and the outdoor MBS is represented by $j = 0$. The pathloss between FUE k_l connected to FAP l and the MBS $j = 0$ is given by [18]:

$$PL_{k_l,j,\mathrm{dB}} = 15.3 + 37.6\log_{10} d_{\mathrm{out},k_l,j} + 0.3 d_{\mathrm{in},k_l,j} + qL_{\mathrm{iw}} + L_{\mathrm{ow}} \tag{7.2}$$

where $d_{\mathrm{out},k_l,j}$ is the distance traveled outdoor between the MBS and the building external wall, $d_{\mathrm{in},k_l,j}$ is the indoor traveled distance between the building wall and FUE k_l, and L_{ow} is an outdoor-indoor penetration loss (loss incurred by the outdoor signal to penetrate the building). It is set to $L_{\mathrm{ow}} = 20$ dB [18]. In this chapter, the MBS is considered to be located at a distance d_{BS} from the building. Thus, the indoor distance can be considered negligible compared to the outdoor distance. Furthermore, the MBS is assumed to be facing the building of Fig. 7.3, such that $q = 0$

can be used. Thus, the outdoor-indoor propagation model of (7.2) becomes:

$$PL_{k_l,j,\mathrm{dB}} = 15.3 + 37.6 \log_{10} d_{k_l,j} + L_{\mathrm{ow}} \tag{7.3}$$

Taking into account fading fluctuations in addition to pathloss, the channel gain between FUE k_l and FAP/MBS j can be expressed as:

$$H_{k_l,i,j,\mathrm{dB}} = -PL_{k_l,j,\mathrm{dB}} + \xi_{k_l,j} + 10 \log_{10} F_{k_l,i,j} \tag{7.4}$$

where the first factor captures propagation loss, according to (7.1) or (7.2)-(7.3). The second factor, $\xi_{k_l,j}$, captures log-normal shadowing with zero-mean and a standard deviation σ_ξ (set to $\sigma_\xi = 8$ dB in this chapter), whereas the last factor, $F_{k_l,i,j}$, corresponds to Rayleigh fading power between FUE k_l and FAP or BS j over RB i, with a Rayleigh parameter b such that $E\{|b|^2\} = 1$. It should be noted that fast Rayleigh fading is assumed to be approximately constant over the subcarriers of a given RB, and independent identically distributed (iid) over RBs.

7.3.2 Calculation of the Data Rates

Letting $\mathscr{I}_{\mathrm{sub},k_l}$ and $\mathscr{I}_{\mathrm{RB},k_l}$ be the sets of subcarriers and RBs, respectively, allocated to FUE k_l in femtocell l, N_{RB} the total number of RBs, L the number of FAPs, K_l the number of FUEs connected to FAP l, $P_{i,l}$ the power transmitted over subcarrier i by FAP l, $P_{l,\max}$ the maximum transmission power of FAP l, and R_{k_l} the achievable data rate of FUE k_l in femtocell l, then the OFDMA throughput of FUE k_l in femtocell l is given by:

$$R_{k_l}(\mathbf{P_l}, \mathscr{I}_{\mathrm{sub},k_l}) = \sum_{i \in \mathscr{I}_{\mathrm{sub},k_l}} B_{\mathrm{sub}} \cdot \log_2(1 + \beta \gamma_{k_l,i,l}) \tag{7.5}$$

where B_{sub} is the subcarrier bandwidth expressed as $B_{\mathrm{sub}} = \frac{B}{N_{\mathrm{sub}}}$, with B the total usable bandwidth, and N_{sub} the total number of subcarriers. In (7.5), β refers to the signal to noise ratio (SNR) gap. It indicates the difference between the SNR needed to achieve a certain data transmission rate for a practical M-QAM (quadrature amplitude modulation) system and the theoretical limit (Shannon capacity) [19]. It is given by $\beta = \frac{-1.5}{\ln(5P_b)}$, where P_b denotes the target bit error rate (BER), set to $P_b = 10^{-6}$ in this chapter.

In addition, in (7.5), $\mathbf{P_l}$ represents a vector of the transmitted power on each subcarrier by FAP/MBS l, $P_{i,l}$. In this chapter, the transmit power is considered to be equally allocated over the subcarriers. Hence, for all i, we have $P_{i,l} = \frac{P_{l,\max}}{N_{\mathrm{sub}}}$.

The signal to interference plus noise ratio (SINR) of FUE k_l over subcarrier i in cell l in the DL, $\gamma_{k_l,i,l}$, is expressed as:

$$\gamma_{k_l,i,l} = \frac{P_{i,l} H_{k_l,i,l}}{I_{i,k_l} + \sigma^2_{i,k_l}} \tag{7.6}$$

where σ^2_{i,k_l} is the noise power over subcarrier i in the receiver of FUE k_l, and I_{i,k_l} is the interference on subcarrier i measured at the receiver of FUE k_l. The expression of the interference is given by:

$$I_{i,k_l} = \sum_{j\neq l, j=0}^{L} \left(\sum_{k_j=1}^{K_j} \alpha_{k_j,i,j} \right) \cdot P_{i,j} H_{k_l,i,j} \tag{7.7}$$

In (7.7), K_j is the number of FUEs served by FAP j, and $\alpha_{k_j,i,j}$ is a binary variable representing the exclusivity of subcarrier allocation: $\alpha_{k_j,i,j} = 1$ if subcarrier i is allocated to FUE k_j in cell j, i.e., $i \in \mathscr{I}_{\text{sub},k_j}$, and $\alpha_{k_j,i,j} = 0$ otherwise. In fact, in each cell, an LTE RB, along with the subcarriers constituting that RB, can be allocated to a single FUE at a given TTI. Consequently, the following is verified in each cell j:

$$\sum_{k_j=1}^{K_j} \alpha_{k_j,i,j} \leq 1 \tag{7.8}$$

The term corresponding to $j = 0$ in (7.7) represents the interference from the MBS, whereas the terms corresponding to $j = 1$ to $j = L$ represent the interference from the other FAPs in the building.

7.4 Network Utility Maximization

In this section, the problem formulation for maximizing the network utility is presented. In addition, different utility metrics leading to different QoS objectives are presented and discussed.

7.4.1 Problem Formulation

With $U^{(l)}$ and U_{k_l} denoting the utility of FAP l and FUE k_l, respectively, such that $U^{(l)} = \sum_{k_l=1}^{K_l} U_{k_l}$, then the objective is to maximize the total utility in the network of Fig. 7.2, $\sum_{l=1}^{L} U^{(l)}$:

$$\max_{\alpha_{k_l,i,l}, P_{i,l}} U_{\text{tot}} = \sum_{l=1}^{L} U^{(l)} \tag{7.9}$$

Subject to:

$$\sum_{i=1}^{N_{\text{sub}}} P_{i,l} \leq P_{l,\max}; \forall l = 1, ..., L \tag{7.10}$$

$$\sum_{k_l=1}^{K_l} \alpha_{k_l,i,l} \leq 1; \forall i = 1, ..., N_{\text{sub}}; \forall l = 1, ..., L \tag{7.11}$$

The constraint in (7.10) indicates that the transmit power cannot exceed the maximum FAP transmit power, whereas the constraint in (7.11) corresponds to the exclusivity of subcarrier allocation in each femtocell, since in each LTE cell, a subcarrier can be allocated at most to a unique user at a given scheduling instant. Different utility functions depending on the FUEs' data rates are described next.

7.4.2 Utility Selection

The utility metrics investigated include Max C/I, proportional fair (PF), and Max-Min utilities. The impact of their implementation on the sum-rate, geometric mean, maximum and minimum data rates in the network is studied in Section 7.7.1 using the Algorithm of Section 7.5.

7.4.2.1 Max C/I Utility

Letting the utility equal to the data rate $U_k = R_k$, the formulation in (7.9) becomes a greedy maximization of the sum-rate in the network. This approach is known in the literature as Max C/I. However, in this case, FUEs with favorable channel and interference conditions will be allocated most of the resources and will achieve very high data rates, whereas FUEs suffering from higher propagation losses and/or interference levels will be deprived from RBs and will have very low data rates.

7.4.2.2 Max-Min Utility

Due to the unfairness of Max C/I resource allocation, the need for more fair utility metrics arises. Max-Min utilities are a family of utility functions attempting to maximize the minimum data rate in the network, e.g., [20, 21]. A vector $\mathbf{R}$ of FUE data rates is Max-Min fair if and only if, for each k, an increase in R_k leads to a decrease in R_j for some j with $R_j < R_k$ [20]. By increasing the priority of FUEs having lower rates, Max-Min utilities lead to more fairness in the network. It was shown that Max-Min fairness can be achieved by utilities of the form [21]:

$$U_k(R_k) = -\frac{R_k^{-a}}{a}, a > 0 \tag{7.12}$$

where the parameter a determines the degree of fairness. Max-Min fairness is attained when $a \to \infty$ [21]. We use $a = 10$ in this chapter. However, enhancing the worst case performance could come at the expense of FUEs with good channel conditions (and who could achieve high data rates) that will be unfavored by the RRM algorithms in order to increase the rates of worst case FUEs. A tradeoff between

Max C/I and Max-Min RRM can be achieved through proportional fair (PF) utilities, described next.

7.4.2.3 Proportional Fair Utility

A tradeoff between the maximization of the sum rate and the maximization of the minimum rate could be the maximization of the geometric mean data rate. The geometric mean data rate for K FUEs is given by:

$$R^{(\mathrm{gm})} = \left(\prod_{k=1}^{K} R_k \right)^{1/K} \tag{7.13}$$

The metric (7.13) is fair, since an FUE with a data rate close to zero will make the whole product in $R^{(\mathrm{gm})}$ go to zero. Hence, any RRM algorithm maximizing $R^{(\mathrm{gm})}$ would avoid having any FUE with very low data rate. In addition, the metric (7.13) will reasonably favor FUEs with good wireless channels (capable of achieving high data rate), since a high data rate will contribute in increasing the product in (7.13).

To be able to write the geometric mean in a sum-utility form as in (7.9), it can be noted that maximizing the geometric mean in (7.13) is equivalent to maximizing the product, which is equivalent to maximizing the sum of logarithms:

$$\begin{aligned} \max \prod_{k=1}^{K} R_k \Longleftrightarrow \max \ln \left(\prod_{k=1}^{K} R_k \right) \\ = \max \sum_{k=1}^{K} \ln(R_k) \end{aligned} \tag{7.14}$$

Consequently, the algorithmic implementation of (7.14) can be handled by the algorithm of Section 7.5, by using, in that algorithm, $U_k = \ln(R_k)$ as the utility of FUE k, where ln represents the natural logarithm. Maximizing the sum of logarithms in (7.14) is equivalent to maximizing the product and is easier to implement numerically. Hence, letting $U = \ln(R)$ provides proportional fairness [21, 22].

7.4.2.4 QoS-based Utility

The Max C/I, proportional fair (PF), and Max-Min utilities reflect the network performance, but do not indicate if a specific FUE has achieved a desired QoS level or not. For the green network operation, maximizing sum-rate or the minimum rate by itself could prevent switching off certain FAPs. Instead, the objective in this case would be to maximize the number of FUEs achieving their QoS requirements. Resources allocated to increase the data rates beyond these requirements would be redundant. Therefore, in this section, we propose a utility that reflects the number of FUEs achieving a target data rate R_{th}, or how close they are to achieve it.

The utility function used for this purpose is expressed as follows:

$$U_{k_l} = 1_{R_{k_l} \geq R_{\text{th}}} + 1_{R_{k_l} < R_{\text{th}}} \frac{R_{k_l}}{R_{\text{th}}} \tag{7.15}$$

In (7.15), the notation $1_{(\text{Condition})}$ is used such that $1_{(\text{Condition})} = 1$ if condition is verified, and $1_{(\text{Condition})} = 0$ if the condition is not verified. This utility aims to maximize the number of FUEs who exceed their target data rate threshold R_{th} (first term in (7.15)), or, if this is not achievable, reach a data rate as close as possible to R_{th} (second term in (7.15), which corresponds to the fraction of R_{th} achieved by the FUE). This utility is used with the Algorithm of Section 7.6 in order to obtain the results of Section 7.7.2.

7.5 Centralized RRM Algorithm

To perform the maximization of (7.9), we use the utility maximization algorithm, Algorithm 1, described in this section. This algorithm was first presented by the author in [23]. In this chapter, the energy efficiency aspects are added and investigated through Algorithm 2 presented in Section 7.6, and the two algorithms are compared in the results section. Algorithm 1 can be applied with a wide range of utility functions, thus being able to achieve various objectives, with each objective represented by a certain utility function. Hence, it can be used for max C/I, PF, and Max-Min RRM, with the utilities derived in Section 7.4.2.

Lines 1-8 in Algorithm 1 are used for initialization. The loop in lines 10-21 determines the network utility enhancement that can be achieved by each (FUE, RB) allocation. The allocation leading to maximum enhancement (Line 22) is performed if it leads to an increase in network utility (Lines 23-30). After each allocation, the interference levels in the network vary. Hence, interference and data rates are updated and the novel utilities are computed. The process is repeated until no additional improvement can be obtained (Lines 9-34), with $I_{\text{Improvement}}$ being an indicator variable tracking if an improvement in network utility has been achieved ($I_{\text{Improvement}} = 1$) or not ($I_{\text{Improvement}} = 0$).

Algorithm 1 is implemented by the central controller in the scenario described in Section 7.3. In this chapter, one FUE is considered to be active per femtocell, without loss of generality. In the case where each FAP performs RRM in a distributed way (without wired connections to a central controller), then the maximization of the three utility types in each femtocell is achieved by allocating all the RBs of a given FAP to the active FUE. In fact, in this case, there would be no information about the channel gains and interference levels in the other femtocells. Thus, it makes sense for each FAP to try to maximize the QoS of its served FUE by allocating all available resources to that FUE. For a given FAP l, this corresponds, simultaneously, to maximizing the sum rate, maximizing the logarithm of the rate, and maximizing the minimum rate (In fact, with one FUE k_l present, R_{k_l} is the only rate and thus would correspond to the sum rate, the minimum rate, and the geomet-

Algorithm 1 Utility Maximization Algorithm

for all FAP l and FUE k_l **do**
  for all RB j **do**
    $\alpha^{\text{old}}_{k_l,j} = 0$
    $U^{\text{old}}_{k_l}(\alpha^{\text{old}}) = 0$
  end for
end for
$U^{\text{old}}_{\text{tot}} = \sum_{l=1}^{L} \sum_{k_l=1}^{K_l} U^{\text{old}}_{k_l}(\alpha^{\text{old}})$
$I_{\text{Improvement}} = 1$
while $I_{\text{Improvement}} = 1$ **do**
  for all FAP l and FUE k_l **do**
    for all RB j **do**
      $\alpha^{\text{new}} = \alpha^{\text{old}}$
      $\alpha^{\text{new}}_{k_l,j} = 1$
      for all FAP m and FUE k_m **do**
        Calculate the interference and achievable data rates in the network
        Calculate $U^{\text{new}}_{k_m}(\alpha^{\text{new}})$
      end for
      $U^{\text{new}}_{\text{tot}} = \sum_{l=1}^{L} \sum_{k_l=1}^{K_l} U^{\text{new}}_{k_l}(\alpha^{\text{new}})$
      $\delta_{k_l,j} = U^{\text{new}}_{\text{tot}} - U^{\text{old}}_{\text{tot}}$
    end for
  end for
  Find $(k^*, l^*, j^*) = \arg\max_{k,l,j} \delta_{k_l,j}$
  if $\delta_{k^*_{l^*},j^*} > 0$ **then**
    $\alpha^{\text{old}}_{k^*_{l^*},j^*} = 1$
    for all FAP m and FUE k_m **do**
      Calculate the interference and achievable data rates in the network
      Calculate $U^{\text{old}}_{k_m}(\alpha^{\text{old}})$
    end for
    $U^{\text{old}}_{\text{tot}} = \sum_{l=1}^{L} \sum_{k_l=1}^{K_l} U^{\text{old}}_{k_l}(\alpha^{\text{old}})$
    $I_{\text{Improvement}} = 1$
  else
    $I_{\text{Improvement}} = 0$
  end if
end while

ric mean data rate in cell l). This uncoordinated allocation will lead to an increase in interference levels, and to an overall degradation of performance in the network, as shown by the results of Section 7.7.

It should be noted that Algorithm 1 allocates the resources of a given FAP exclusively to the FUE served by that FAP, i.e., it supports closed access operation, although it optimizes the performance by providing centralized control over the RRM process. In a green networking scenario, certain FAPs can be switched-off and their FUEs served by other FAPs in order to save energy. Hence, an algorithm with open-

Algorithm 2 RRM algorithm implemented at a given FAP l

for $N_{\text{rounds}} = 1$ to $\text{Max}_{\text{Rounds}}$ **do**
  for $l = 1$ to L **do**
    $\delta_l = 0$
  end for
  Find $l = \arg\min_{j;\xi_j=1,\delta_j=0} \sum_{k_j=1}^{K_j} \sum_{i=1}^{N_{\text{RB}}} \alpha_{k_j,i,j}$
  $k_l = 0$
  $\delta_l = 1$
  HO_OK = 1
  while $k_l < K_l$ AND HO_OK = 1 **do**
    $k_l = k_l + 1$
    Find $j^* = \arg\max_{j;\xi_j=1} \sum_{i=1}^{N_{\text{RB}}} \gamma_{k_l,i,j}$
    $N_{\text{Attempts}} = 0$
    $R_{k_l} = 0$
    while $(R_{k_l} < R_{\text{th}})$ AND $(\sum_{i=1}^{N_{\text{RB}}} \alpha_{k_l,i,j^*} < N_{\text{RB}})$ AND $(N_{\text{Attempts}} < \text{Max}_{\text{Attempts}})$ **do**
      $N_{\text{Attempts}} = N_{\text{Attempts}} + 1$
      Find $i^* = \arg\max_{i;\alpha_{k_l,i,j^*}=0} \gamma_{k_l,i,j^*}$
      Allocate RB i^* to FUE k_l: $\alpha_{k_l,i^*,j^*} = 1$
      Calculate the rate of FUE k_l over RB i^*: R_{k_l,i^*}
      Set $R_{k_l} = R_{k_l} + R_{k_l,i^*}$
    end while
    if $R_{k_l} \geq R_{\text{th}}$ **then**
      for all RB i such that $\alpha_{k_l,i,l} = 1$ **do**
        $\alpha_{k_l,i,l} = 0$
      end for
      HO_OK = 1
    else
      for all RB i such that $\alpha_{k_l,i,j^*} = 1$ **do**
        $\alpha_{k_l,i,j^*} = 0$
      end for
      HO_OK = 0
    end if
  end while
  if HO_OK = 1 AND $\sum_{k_l=1}^{K_l} \sum_{i=1}^{N_{\text{RB}}} \alpha_{k_l,i,l} = 0$ **then**
    $\xi_l = 0$
  end if
end for

access operation, allowing FAP switch off while meeting the QoS requirements of FUEs is required. Such an algorithm is presented in Section 7.6.

7.6 Green FAP Switching Algorithm

To perform centralized energy efficient operation of the femtocell network, the proposed Algorithm 2, described in this section, is used. Algorithm 2 is implemented by the central controller in the scenario described in Section 7.3. In this chapter, one FUE is considered to be active per femtocell, without loss of generality, since Algo-

rithm 2 is applicable with any number of FUEs per femtocell. An FUE is considered to be successfully served if it achieves a data rate above a defined threshold R_{th}.

In the algorithm, δ_l is a tracking parameter used to track if an attempt has been made to switch off FAP l. It is set to $\delta_l = 1$ if an attempt was made and to $\delta_l = 0$ otherwise. ξ_l is a parameter indicating if FAP l is switched on or off. It is set to $\xi_l = 1$ if the FAP is active and to $\xi_l = 0$ if it is switched off. In this chapter, we set $\text{Max}_{\text{Rounds}} = L$ and $\text{Max}_{\text{Attempts}} = N_{\text{RB}}$.

The algorithm finds the FAP that has the lowest load, with the load defined in this chapter as the number of allocated RBs in the FAP (Line 5). It then makes an attempt to switch off this FAP by moving its served FUEs to neighboring active FAPs (Loop at Lines 9-32). The algorithm finds for each FUE, the best serving FAP other than the current FAP l, in terms of best average SINR (Line 11). If the FUE can be successfully handed over to the target FAP (and it can achieve its target rate after resource allocation at Lines 14-20), it is handed over and the handover parameter HO_OK is set to 1 (Lines 21-25). If at least one FUE cannot be handed over, HO_OK is set to 0 and FAP l remains on after freeing any reserved RBs in the target FAP (Lines 27-30). When all FUEs are handed over successfully, FAP l can be switched off (Lines 33-35). Otherwise, if at least one FUE was not served successfully, FAP l remains active.

7.7 Results and Discussion

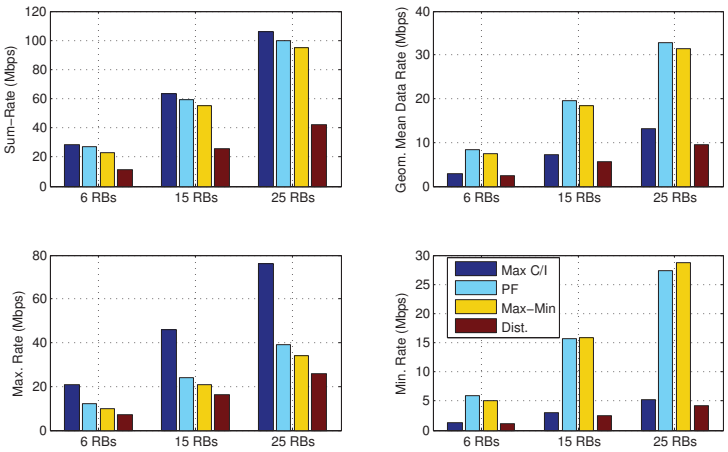

Fig. 7.4 Results in the case of one floor (three femtocells).

This section presents the Matlab simulation results obtained by implementing the proposed approach under the system model of Section 7.3. We consider a building as shown in Fig. 7.2. Three apartments per floor are assumed, with one active FUE per

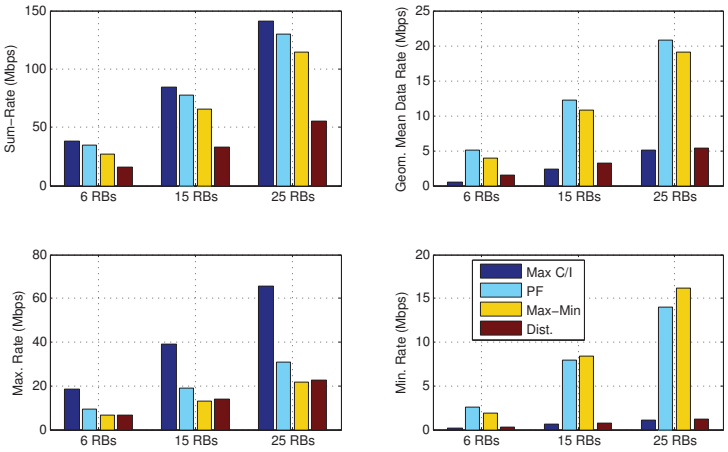

Fig. 7.5 Results in the case of two floors (six femtocells).

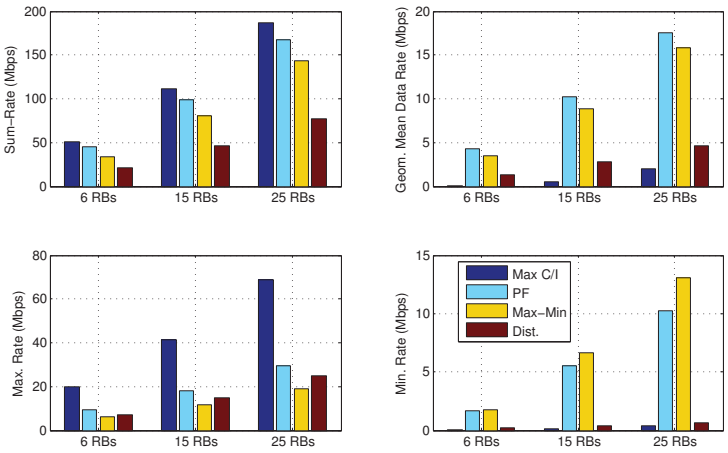

Fig. 7.6 Results in the case of three floors (nine femtocells).

apartment using the FAP to access the network (assuming one FAP per apartment). The maximum FAP transmit power is set to 1 Watt, whereas the transmit power of the macro BS is set to 10 Watts.

7.7.1 Results of Centralized RRM with all the FAPs Active

This section presents the results of implementing Algorithm 1 described in Section 7.5 when all the FAPs are active. Scenarios with one floor only (three apartments on ground floor), two floors (six apartments), and three floors (nine apart-

ments) are investigated, with the results shown in Figs. 7.4, 7.5, and 7.6, respectively.

The figures show that max C/I scheduling leads to the highest sum-rate in the network. However, this comes at the expense of fairness, as it can be seen from the geometric mean results of max C/I. In fact, the bottom subfigures of Figs. 7.4 to 7.6 show that max C/I enhances the maximum rate in the network, by allocating most of the resources to the FUE having the best channel and interference conditions, while depriving other FUEs from sufficient resources, thus leading to unfairness, as shown by the minimum rate plots. On the other hand, PF scheduling maximizes the geometric mean for all the investigated scenarios. Clearly, the minimum rates achieved with PF indicate that a PF utility is significantly more fair than max C/I. The results of Max-Min scheduling also show a fair performance. In fact, Max-Min resource allocation leads to maximizing the minimum rate in the network for almost all the studied scenarios, except in the case of one and two floors with six RBs, where it is slightly outperformed by PF. This is due to the approximation performed by taking, in (7.12), $a = 10$ instead of $a = \infty$. When the number of resources increases to 15 and 25 RBs, the algorithm has additional flexibility to implement RRM with Max-Min such that the minimum rate is maximized compared to the other methods. It can also be noted that Max-Min scheduling leads to a geometric mean performance that is reasonably close to that of PF scheduling, indicating that it also enhances overall fairness in the network. Figs. 7.4 to 7.6 also show that, as expected, the data rates increase for all the studied metrics when the number of RBs increases.

Comparing the joint wired/wireless case to the distributed scenario where each FAP performs RRM independently without centralized control, it can be seen that the distributed scenario is outperformed by the integrated wired/wireless approach for all the investigated metrics: Max C/I leads to a higher sum-rate, PF leads to a higher geometric mean, and Max-Min leads to a higher minimum rate. This is due to the fact that with distributed RRM, a FAP is not aware of the interference conditions to/from other FAPs and FUEs. This leads to a severe performance degradation, as can be seen in Figs. 7.4 to 7.6, although all the RBs of a given FAP are allocated to the FUE served by that FAP.

7.7.2 Results of the Green Network Operation with FAP On/Off Switching

This section presents the simulation results, considering the scenario of Fig. 7.2, with different values for R_{th} and the available LTE bandwidth. The following methods are compared:

- The centralized scheduling algorithm presented in Section 7.5. It assumes each FAP serves only its corresponding FUEs without taking energy efficiency into account. But the resource allocation is performed by the central controller, which allows to avoid interference.

Table 7.1 Average Data Rates (Mbps)

	Centralized	**Green Centralized**	**Selfish**
$N_{\text{RB}} = 15$ $R_{\text{th}} = 2$ Mbps	2.74	3.01	5.25
$N_{\text{RB}} = 15$ $R_{\text{th}} = 5$ Mbps	6.01	6.06	5.25
$N_{\text{RB}} = 15$ $R_{\text{th}} = 7$ Mbps	7.64	7.18	5.25
$N_{\text{RB}} = 15$ $R_{\text{th}} = 10$ Mbps	9.44	8.94	5.25
$N_{\text{RB}} = 25$ $R_{\text{th}} = 5$ Mbps	6.09	6.14	8.54
$N_{\text{RB}} = 25$ $R_{\text{th}} = 7$ Mbps	7.82	7.87	8.54
$N_{\text{RB}} = 25$ $R_{\text{th}} = 10$ Mbps	10.94	10.91	8.54
$N_{\text{RB}} = 50$ $R_{\text{th}} = 10$ Mbps	11.00	11.04	15.90

- The "selfish" approach, where each FBS allocates all its RBs to the FUE it is serving, regardless of the allocations in other cells. This scenario assumes neither centralized control, nor any form of coordination between FAPs. Thus, it would be logical for each FAP to allocate all resources to its served FUEs, given that no other coordination or interference information is available.
- The approach proposed in Algorithm 2, where, starting from an initial allocation without energy efficiency obtained by implementing Algorithm 1, the proposed Algorithm 2 implements centralized FAP switching off after offloading FUEs to active FAPs that can maintain their QoS.

In this section, we use a capped capacity formula in order to limit the possibility of FUEs to achieve their target rate:

$$R_{k_l}(\mathbf{P_1}, \mathscr{I}_{\text{sub},k_l}) = \max\Big(\sum_{i\in\mathscr{I}_{\text{sub},k_l}} B_{\text{sub}} \cdot \log_2(1+\beta\gamma_{k_l,i,l}), R_{\max}\Big) \tag{7.16}$$

Compared to (7.5), the expression in (7.16) is a capped Shannon formula; i.e., the data rate is not allowed to exceed the maximum limit $R_{\max}$ that can be reached using

Table 7.2 Geometric Mean Data Rates (Mbps)

	Centralized	**Green Centralized**	**Selfish**
$N_{\text{RB}} = 15$ $R_{\text{th}} = 2$ Mbps	2.15	2.94	2.83
$N_{\text{RB}} = 15$ $R_{\text{th}} = 5$ Mbps	5.83	6.00	2.83
$N_{\text{RB}} = 15$ $R_{\text{th}} = 7$ Mbps	7.46	6.57	2.83
$N_{\text{RB}} = 15$ $R_{\text{th}} = 10$ Mbps	8.84	6.01	2.83
$N_{\text{RB}} = 25$ $R_{\text{th}} = 5$ Mbps	5.92	6.07	4.66
$N_{\text{RB}} = 25$ $R_{\text{th}} = 7$ Mbps	7.70	7.83	4.66
$N_{\text{RB}} = 25$ $R_{\text{th}} = 10$ Mbps	10.84	10.78	4.66
$N_{\text{RB}} = 50$ $R_{\text{th}} = 10$ Mbps	10.91	11.01	8.56

practical modulation and coding schemes (MCS) in LTE. This limit is determined as follows:

$$R_{\max} = \frac{r_n \cdot N_{\text{RB}}^{(k_l)} \cdot N_{\text{SC}}^{\text{RB}} \cdot N_{\text{Symb}}^{\text{SC}} \cdot N_{\text{Slot}}^{\text{TTI}}}{T_{\text{TTI}}}, \tag{7.17}$$

where r_n is the rate in bits/symbol corresponding to the MCS used over the subcarriers of the RBs allocated to the FUE. $R_{\max}$ is obtained with $r_n = 6$ corresponding to uncoded 64-QAM, the highest MCS used in LTE. In addition, $N_{\text{RB}}^{(k_l)}$ is the number of RBs allocated to k_l, $N_{\text{SC}}^{\text{RB}}$ is the number of subcarriers per RB (equal to 12 in LTE), $N_{\text{Symb}}^{\text{SC}}$ is the number of symbols per subcarrier during one time slot (set to six or seven in LTE, depending whether an extended cyclic prefix is used or not), $N_{\text{Slot}}^{\text{TTI}}$ is the number of time slots per TTI (two 0.5ms time slots per TTI in LTE), and T_{TTI} is the duration of one TTI (1ms in LTE) [16].

We use the utility (7.15) with both Algorithms 1 and 2. The average data rate results are shown in Table 7.1. However, the average rate results alone can be misleading. In fact, when an FUE A has a very high data rate while another FUE B has a very poor data rate, the average might still be high, but the poor performance of FUE B is masked by the high rate of FUE A. Using the geometric mean results provides a better indication of fairness. The geometric mean data rate results are presented in

Table 7.3 Fraction of FUEs in Outage

	Centralized	**Green Centralized**	**Selfish**
$N_{\text{RB}} = 15$ $R_{\text{th}} = 2$ Mbps	0.16	0.0	0.36
$N_{\text{RB}} = 15$ $R_{\text{th}} = 5$ Mbps	0.11	0.0	0.62
$N_{\text{RB}} = 15$ $R_{\text{th}} = 7$ Mbps	0.15	0.13	0.73
$N_{\text{RB}} = 15$ $R_{\text{th}} = 10$ Mbps	0.55	0.44	0.83
$N_{\text{RB}} = 25$ $R_{\text{th}} = 5$ Mbps	0.11	0	0.46
$N_{\text{RB}} = 25$ $R_{\text{th}} = 7$ Mbps	0.11	0	0.57
$N_{\text{RB}} = 25$ $R_{\text{th}} = 10$ Mbps	0.10	0.01	0.68
$N_{\text{RB}} = 50$ $R_{\text{th}} = 10$ Mbps	0.11	0	0.49

Table 7.2. In addition, Table 7.3 shows the fraction of FUEs in outage, i.e. the number of FUEs that did not achieve R_{th} divided by the total number of FUEs. Table 7.4 shows the fraction of FAPs that are active in order to serve the FUEs. Naturally, the centralized and selfish cases have all their values equal to 1, since 100% of the FAPs are active. Table 7.5 shows the value of the utility function (7.15).

Tables 7.1-7.5 show that the centralized scheduling approach and the centralized green approach significantly outperform the selfish method, especially in terms of fairness and outage. The results of Table 7.4 indicate that the proposed green method of Algorithm 2 is achieving significant energy savings, as it is using only one or two FAPs to serve the nine FUEs (indeed, the value 0.11 corresponds to the ratio $1/9$). This is an interesting result, since it indicates that FUEs in neighboring apartments can be successfully served by a single FAP, which saves around 90 % of FAP energy consumption.

Comparing the results of Algorithm 1 to Algorithm 2, Tables 7.1, 7.2, and 7.5 show that they have a comparable performance, with one being slightly better than the other, or vice versa. However, interestingly, Table 7.3 shows that Algorithm 2 always leads to better outage performance. This is explained by the fact, that, although fully centralized and using all FAPs, Algorithm 1 operates under the constraint that a FAP serves only the FUEs in its apartment. Hence, although centralized control

Table 7.4 Fraction of Active FAPs

	Centralized	**Green Centralized**	**Selfish**
$N_{RB} = 15$ $R_{th} = 2$ Mbps	1	0.11	1
$N_{RB} = 15$ $R_{th} = 5$ Mbps	1	0.11	1
$N_{RB} = 15$ $R_{th} = 7$ Mbps	1	0.12	1
$N_{RB} = 15$ $R_{th} = 10$ Mbps	1	0.21	1
$N_{RB} = 25$ $R_{th} = 5$ Mbps	1	0.11	1
$N_{RB} = 25$ $R_{th} = 7$ Mbps	1	0.11	1
$N_{RB} = 25$ $R_{th} = 10$ Mbps	1	0.11	1
$N_{RB} = 50$ $R_{th} = 10$ Mbps	1	0.11	1

allows mitigating interference and a joint selection of suitable RBs in all FAPs, this approach disregards certain scenarios where fading is constructive with other FAPs, leading occasionally to better channels when an FUE is served by the FAP of another apartment. With the proposed green method, this constraint is relaxed since the purpose is to offload FUEs in order to switch FAPs off. Furthermore, switching off certain FAPs for energy efficiency has the desirable side effect of reducing the interference in the network, due to shutting down some (or in the simulated scenario, most) of the transmitters. Indeed, Algorithm 2 starts from an initial implementation of Algorithm 1, followed by an enhancement operation consisting of FAP switch off in order to reduce the energy consumption in the network.

7.8 Conclusions

In this chapter, femtocell networks designed for supporting IoT traffic were studied. Radio resource management and green operation in LTE and beyond (5G) femtocell networks with centralized control was investigated. The studied scenario consisted of an integrated wired/wireless system, where the femtocell access points are con-

Table 7.5 Normalized Utility

	Centralized	**Green Centralized**	**Selfish**
$N_{RB} = 15$ $R_{th} = 2$ Mbps	0.90	1.0	0.79
$N_{RB} = 15$ $R_{th} = 5$ Mbps	0.97	1.0	0.62
$N_{RB} = 15$ $R_{th} = 7$ Mbps	0.97	0.92	0.53
$N_{RB} = 15$ $R_{th} = 10$ Mbps	0.90	0.76	0.44
$N_{RB} = 25$ $R_{th} = 5$ Mbps	0.98	1	0.72
$N_{RB} = 25$ $R_{th} = 7$ Mbps	0.98	1	0.65
$N_{RB} = 25$ $R_{th} = 10$ Mbps	0.98	0.99	0.56
$N_{RB} = 50$ $R_{th} = 10$ Mbps	0.99	1	0.70

trolled by a single entity. This permits performing joint radio resource management in a centralized and controlled way in order to enhance the quality of service performance for all users in the networks. It also allows an energy efficient operation of the network by switching off redundant femtocells whenever possible. Two algorithms were proposed and analyzed. The first one is a utility maximizing radio resource management algorithm. It was used to maximize different utility functions leading to different target objectives in terms of network sum-rate, fairness, and enhancing the worst-case performance in the network. The second algorithm is FAP switch off algorithm, implemented at the central controller. The joint wired/wireless resource management approach was compared to the distributed resource management case, where each femtocell acts as an independent wireless network unaware of the channel and interference conditions with the other cells. The integrated wired/wireless approach led to significant gains compared to the wireless only case, and the performance tradeoffs between the various utility functions were analyzed and assessed. The results of the green algorithm showed significant energy savings while satisfying QoS requirements.

References

1. Y.-K. Chen, "Challenges and opportunities of internet of things", *in Proc. of the Asia and South Pacific Design Automation Conference (ASP-DAC)*, pp. 383–388, Sydney, Australia, January-February 2012.
2. E. Yaacoub and A. Abu-Dayya, "Automatic Meter Reading in the Smart Grid Using Contention Based Random Access over the Free Cellular Spectrum", *Computer Networks (Elsevier)*, Vol. 59, pp. 171–183, February 2014.
3. E. Yaacoub and A. Kadri, "LTE Radio Resource Management for Real-Time Smart Meter Reading in the Smart Grid", *IEEE ICC 2015 - Workshop on Green Communications and Networks with Energy Harvesting, Smart Grids, and Renewable Energies*, London, UK, June 2015.
4. J. Lloret, A. Canovas, S. Sendra, and L. Parra, "A Smart Communication Architecture for Ambient Assisted Living", *IEEE Communications Magazine*, vol. 53, no. 1, pp.26–33, January 2015.
5. L. Mainetti, L. Patrono, and A. Vilei, "Evolution of wireless sensor networks towards the internet of things: A survey", *in Proc. of the International Conference on Software, Telecommunications and Computer Networks (SoftCOM)*, pp. 1–6, Split, Croatia, September 2011.
6. I. Bisio, F. Lavagetto, M. Marchese, and A. Sciarrone, "Smartphone-Centric Ambient Assisted Living Platform for Patients Suffering from Co-Morbidities Monitoring", *IEEE Communications Magazine*, vol. 53, no. 1, pp.34–41, January 2015.
7. V. Chandrasekkhar, J. G. Andrews, and A. Gatherer, "Femtocell Networks: A Survey", *IEEE Communications Magazine*, vol. 46, no. 9, pp. 59–67, 2008.
8. D. Knisely, T. Yoshizawa, and F. Favichia, "Standardization of Femtocells in 3GPP", *IEEE Communications Magazine*, vol. 47, no. 9, pp. 68–75, 2009.
9. J. G. Andrews, H. Claussen, M. Dohler, S. Rangan, and M. C. Reed, "Femtocells: Past, Present, and Future", *IEEE Journal on Selected Areas in Communications*, vol. 30, no. 3, pp. 497–508, 2012.
10. V. Chandrasekhar, M. Kountouris, and J. G. Andrews, "Coverage in Multi-Antenna Two-Tier Networks", *IEEE Transactions on Wireless Communications*, vol. 8, no. 10, pp. 5314–5327, 2009.
11. F. Pantisano, M. Bennis, W. Saad, and M. Debbah, "Spectrum Leasing as an Incentive towards Uplink Macrocell and Femtocell Cooperation", *IEEE Journal on Selected Areas in Communications*, vol. 30, no. 3, pp. 617–630, 2012.
12. C. Gussen, V. Belmega, and M. Debbah, "Pricing and Bandwidth Allocation Problems in Wireless Multi-Tier Networks", *in Proc. of Asilomar Conference on Signals Systems and Computers*, pp. 1633–1637, 2011.
13. S.-Y. Lien, C.-C. Tseng, K.-C. Chen, and C.-W. Su, "Cognitive Radio Resource Management for QoS Guarantees in Autonomous Femtocell Networks", *in Proc. of the IEEE International Conference on Communications, (ICC 2010)*, pp. 1–6, 2010.
14. S. Hong, C.-Y. Oh, and T.-J. Lee, "Resource Allocation Method Using Channel Sensing and Resource Reuse for Cognitive Femtocells", *International Journal of Information and Electronics Engineering*, vol. 3, no. 3, pp. 309–312, 2013.
15. M. A. Abdelmonem, M. Nafie, M. H. Ismail, and M. S., El-Soudani, "Optimized Spectrum Sensing Algorithms for Cognitive LTE Femtocells", *EURASIP Journal on Wireless Communications and Networking* vol. 2012, no. 6, 19 pages (Open Access), 2012.
16. 3rd Generation Partnership Project (3GPP), 3GPP TS 36.211 3GPP TSG RAN Evolved Universal Terrestrial Radio Access (E-UTRA) Physical Channels and Modulation, version 12.2.0, Release 12, 2014.
17. 3rd Generation Partnership Project (3GPP), 3GPP TS 36.213 3GPP TSG RAN Evolved Universal Terrestrial Radio Access (E-UTRA) Physical layer procedures, version 12.2.0, Release 12, 2014.
18. Qualcomm Inc., 3GPP TSG-RAN WG1 #72 R1-130598, Agenda item: 7.3.7, "Channel Models for D2D Deployments", St. Julian's, Malta, 2013.

19. X. Qiu, and K. Chawla, “On the Performance of Adaptive Modulation in Cellular Systems”, *IEEE Transactions on Communications*, vol. 47, no. 6, pp. 884–895, 1999.
20. J.-Y. Le Boudec, “Rate adaptation, Congestion Control and Fairness: A Tutorial”, Tech. Report, Ecole Polytechnique Federale de Lausanne (EPFL), Lausanne, Switzerland, 2008.
21. G. Song, and Y. Li, “Cross-Layer Optimization for OFDM Wireless Networks-Part I: Theoretical Framework”, *IEEE Transactions on Wireless Communications*, vol. 4, no. 2, pp. 614–624, 2005.
22. E. Yaacoub and Z. Dawy, “Resource Allocation in Uplink OFDMA Wireless Systems: Optimal Solutions and Practical Implementations”, John Wiley and Sons / IEEE press, NY, ISBN: 978-1-1180-7450-3, 2012.
23. E. Yaacoub, “Radio Resource Management in Integrated Wired/Wireless LTE Femtocell Networks”, *in Proc. of the 12th International Conference on Wired and Wireless Internet Communications*, Paris, France, May 2014.